

AD-A164 927

EXACT CALCULATIONS OF FIRST ORDER CONTRIBUTIONS TO THE
INCOHERENT INTENSI. (U) PENNSYLVANIA STATE UNIV 1/1
UNIVERSITY PARK LAB FOR ELECTROMAGNET.

UNCLASSIFIED

V V VARADAN ET AL. JAN 86 ARO-21825.1-G5

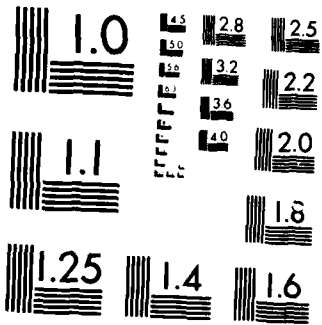
F/G 14/5

NL

END

FILMED

etc.



MICROCOPY RESOLUTION TEST CHART
NATIONAL BUREAU OF STANDARDS 1963-A

Unclassified

2

SECURITY CLASSIFICATION OF THIS PAGE (When Data Entered)

AD-A164 927

REPORT DOCUMENTATION PAGE

READ INSTRUCTIONS BEFORE COMPLETING FORM

REPORT NUMBER ARO 21825.1-GS	2. GOVT ACCESSION NO.	3. RECIPIENT'S CATALOG NUMBER
TITLE (and Subtitle) Exact Calculations of First Order Contributions to the Incoherent Intensity		5. TYPE OF REPORT & PERIOD COVERED Technical Report
AUTHOR(s) Vasundara V. Varadan, Yushieh Ma Vijay K. Varadan		6. PERFORMING ORG. REPORT NUMBER
PERFORMING ORGANIZATION NAME AND ADDRESS Pennsylvania State University		8. CONTRACT OR GRANT NUMBER(s) DAAG29-84-K-0187
CONTROLLING OFFICE NAME AND ADDRESS U. S. Army Research Office Post Office Box 12211 Research Triangle Park, NC 27709		10. PROGRAM ELEMENT, PROJECT, TASK AREA & WORK UNIT NUMBERS
14. MONITORING AGENCY NAME & ADDRESS (if different from Controlling Office)		12. REPORT DATE January, 1986
		13. NUMBER OF PAGES 29
		15. SECURITY CLASS. (of this report) Unclassified
		15a. DECLASSIFICATION/DOWNGRADING SCHEDULE

16. DISTRIBUTION STATEMENT (of this Report)
Approved for public release; distribution unlimited.

17. DISTRIBUTION STATEMENT (of the abstract entered in Block 20, if different from Report)

DTIC ELECTE
S D
FEB 25 1986

18. SUPPLEMENTARY NOTES
The view, opinions, and/or findings contained in this report are those of the author(s) and should not be construed as an official Department of the Army position, policy, or decision, unless so designated by other documentation

19. KEY WORDS (Continue on reverse side if necessary and identify by block number)
Inhomogeneities Non-Spherical Scatterers
Incoherent Intensity
Scatterers
Polarizations **DTIC FILE COPY**

20. ABSTRACT (Continue on reverse side if necessary and identify by block number)
Basic studies have been made on the effect of inhomogeneities - via their geometry, size, material properties, distribution, multiple scattering processes and statistical correlations in position and the effect of aligned versus randomly oriented non-spherical scatterers. Emphasis has been on studies of the second moment of the field fluctuation, namely the incoherent intensity. The effects of completely correlated (identical) scatterers versus partially correlated scatterers (distinct) has been studied as a function of observation angle, non-dimensional wavenumber, and concentration.

20. ABSTRACT CONTINUED

Due to the Specific form of the expressions for the incoherent intensity, the effect of correlations is to decrease the value of the incoherent intensity. Since the correlation contribution is also very much angle dependent, the effects are more in some directions than in others.

**EXACT CALCULATIONS OF FIRST ORDER CONTRIBUTIONS TO THE
INCOHERENT INTENSITY**

Vasundara V. Varadan, Yushieh Ma, and Vijay K. Varadan
Laboratory for Electromagnetic and Acoustic Research
Department of Engineering Science and Mechanics
The Pennsylvania State University
University Park, PA 16802

ARO Contract # DAAG29 - 84 - K - 0187

January, 1986

SUMMARY

Basic studies on the effect of inhomogeneities - via their geometry, size, material properties, distribution, multiple scattering processes and statistical correlations in position and the effect of aligned versus randomly oriented non-spherical scatterers has continued this year. Emphasis has been on studies of the second moment of the field fluctuation, namely the incoherent intensity. The effects of completely correlated (identical) scatterers versus partially correlated scatterers (distinct) has been studied as a function of observation angle, non-dimensional wavenumber, and concentration. Due to the specific form of the expressions for the incoherent intensity, the effect of correlations is to decrease the value of the incoherent intensity. Since the correlation contribution is also very much angle dependent, the effects are more in some directions than in others. In every case both vertical and horizontal polarizations are studied and the differences in the results are discussed. The multipole amplitudes of the effective field exciting each scatterer are explicitly calculated leading to more accurate values of the second moment. It may be recalled that the effective field and the effective propagation constant are calculated in the Quasi Crystalline approximation and include the effects of pair correlation and sequential multiple scattering terms. The so called back scattering enhancement is also investigated, relative to the experimental observations of Kuga and Ishimaru and the theoretical explanations of Tsang and Ishimaru using 'cyclical' diagrams.

CONFIDENTIAL
 INSPECTED
 3

Accession For	
NTIS CRA&I	<input checked="" type="checkbox"/>
DTIC TAB	<input type="checkbox"/>
Unannounced	<input type="checkbox"/>
Justification	
By	
Distribution /	
Availability Codes	
Dist	Avail and/or Special
A-1	

INTRODUCTION

In this paper, a systematic study is made of first order contributions to the second moment or incoherent intensity of the electromagnetic field propagating in a discrete random medium. The second moment, which is traditionally defined as the correlation function of the component of the field fluctuations in any direction \hat{u} , denoted by I_u can be written as

$$I_u = \langle \hat{u} \cdot (\mathbf{E} - \langle \mathbf{E} \rangle) (\mathbf{E} - \langle \mathbf{E} \rangle)^* \cdot \hat{u} \rangle = \langle (\hat{u} \cdot \Delta \mathbf{E}) (\hat{u} \cdot \Delta \mathbf{E})^* \rangle$$

where $\Delta \mathbf{E} = \mathbf{E} - \langle \mathbf{E} \rangle$ is the fluctuation of the electric field. Since the field fluctuations can be expanded in a multiple scattering series each term of which contains sums on all possible scatterers, it is evident that we can divide the resulting terms into two sets, one of which involves considering only those terms in which the same scatterer contributes to a particular order term in each field fluctuation and the other which involves distinct scatterers. This latter set of terms will contribute to the incoherent intensity only if statistical correlations between scatterers are taken into account. The first category of terms are equivalent in spirit to radiative transfer theory since it is essentially the intensity of the field scattered by each scatterer that propagates from one site to another. Even for this set of terms, positional correlations between scatterers should be taken into account at volume fractions exceeding a few %, but these terms contribute to the incoherent intensity even if correlations are neglected.

Neglecting correlations, and modeling the scatterers as dipoles, Tsang and Ishimaru have attempted to explain the back scattering enhancement experimentally observed by Kuga and Ishimaru. It must be pointed out that the experiments were performed at wavelengths comparable to and smaller than the scatterer size, invalidating the dipole approximation used in the theory, and further at the concentrations considered in the experiments, correlation effects cannot be neglected. This will be discussed in greater detail later.

The aim of the study presented here is to make very accurate calculations of the first order contributions to the incoherent intensity. By accurate, we mean that the calculations will be numerically exact up to first order. This is achieved by modeling the single scatterer response by

considering the full T- matrix (multipole field), include the effects of pair correlations to the first order term of the incoherent intensity, and lastly the field incident on a scatterer is modeled as an effective exciting field, which propagates at the effective, complex, frequency dependent wavenumber K , which is first computed in the Quasi Crystalline Approximation (QCA). The multipole amplitudes of the effective exciting field are calculated using the extinction theorem. This is in contrast to previous calculations, when all amplitudes were set to unity. By necessity the calculated intensity is normalized by the incident intensity, the illuminated volume, and the distance of propagation into the scattering volume, to take account of the attenuation that the wave suffers before it is incident on the last scatterer.

Numerical results are presented in various forms, as a function of frequency, observation angle, concentration, polarization of the scattered field, i.e. vertical and horizontal polarizations. An effort was made to separate the contributions to first order scattering, so that the effect of pair correlations is clearly visible. To first order, neglecting correlations, results in the single scattering approximation to the incoherent intensity. The effect of correlations, is to actually reduce the intensity, especially close to the forward direction.

Incoherent Scattered Intensity

The total scattered intensity is directly proportional to the second moment of the scattered field. It is known that the total scattered field is a combination of the average scattered field and the fluctuation of the field due to the random distribution of scatterers, i.e., $u = \langle u \rangle + u'$, the incoherent component of the scattered intensity can be obtained as

$$\langle u' u'^* \rangle = \langle u u^* \rangle - \langle u \rangle \langle u \rangle^* \quad (1)$$

where the angular brackets denote an ensemble average. To first order, that is taking only the single scattering contribution to each scattered field, we obtain

$$\begin{aligned} \langle u' u'^* \rangle &= \langle |u'|^2 \rangle = \langle \sum_j u_j^* \sum_k u_k \rangle - \sum_j \langle u_j \rangle^* \sum_k \langle u_k \rangle \\ &= \sum_{j+k} \sum_k \langle u_j^* u_k \rangle + \sum_j \langle |u_j|^2 \rangle - \sum_j \sum_k \langle u_j \rangle^* \langle u_k \rangle \end{aligned} \quad (2)$$

In the above equation, the subscripts j and k denote the scattered field from the j -th and k -th scatterers, respectively. Subscripted angular brackets denote a conditional ensemble average in the usual manner, where the averaging is done keeping the position of the subscripted scatterer(s) fixed. For scatterers randomly distributed in space, the ensemble averages in Eq. (2) can be written by integrating over the random positions r_j, r_k , etc. of the scatterers. Thus

$$\begin{aligned} \langle |u'|^2 \rangle &= n_0^2 \iint [(N-1/N) \langle u_j^* u_k \rangle_{jk} - \langle u_j \rangle_j^* \langle u_k \rangle_k] dr_j dr_k \\ &+ n_0 \int \langle |u_j|^2 \rangle_j dr_j, \end{aligned} \quad (3)$$

where $n_0 = N/V$, is the number density such that the total number of scatterers, $N \rightarrow \infty$, the volume in which they are distributed, $V \rightarrow \infty$, but n_0 is finite. The second term in the above equation, which is proportional to n_0 is the ordinary single scattering approximation to the incoherent intensity and the magnitude of the incoherent intensity in any direction is proportional to the bistatic cross section of a single scatterer. The first term proportional to n_0^2 is due to the effect of positional correlations between pairs of scatterers.

For sparse concentrations, the scatterers are uncorrelated, and

$$\langle u_j^* u_k \rangle_{jk} \approx \langle u_j \rangle_j^* \langle u_k \rangle_k \quad (4)$$

and the first term of Eq. (3) vanishes.

In order to obtain the incoherent intensity for higher concentrations, the pair correlation function $g(\mathbf{x})$ is taken into consideration. Recently Twersky (1982) has modified Eq. (3) for a dense distribution of scatterers in which. The incoherent intensity has the form:

$$\begin{aligned} \langle |u'|^2 \rangle &= n_0^2 \iint [g(r_j - r_k) - 1] \langle u_j \rangle_j^* \langle u_k \rangle_k dr_j dr_k \\ &+ n_0 \int \langle |u_j|^2 \rangle_j dr_j \end{aligned} \quad (5)$$

Equation (5) is the final form used in our computation. However, a knowledge of the coherent field is still required since the average scattered field $\langle u_j \rangle_j$ is involved in the formalism. In the usual manner, the field scattered by the j -th scatterer is expanded in vector spherical functions, with coefficients f_n^j , which are related to the expansion coefficients of the exciting

field via the T- matrix. Thus,

$$u_j = \sum_n f_n^j \text{Ou} \phi_n (r - r_j) \quad (6)$$

and denoting α_n^j , the coefficients of the exciting field

$$f_n^j = \sum_{n'} T_{nn'} \alpha_n^j \quad (7)$$

The average scattered field $\langle u_j \rangle_j$ holding the j -th scatterer fixed can thus be expressed as

$$\langle u_j \rangle_j = \sum_{n'} T_{nn'} \langle \alpha_n^j \rangle_j \quad (8)$$

In writing Eq. (5), we have used the quasi-crystalline approximation, as explained in the previous section.

The exciting field coefficients α_n^j are initially unknown in Eq. (5). However, the average field $\langle \alpha_n^j \rangle_j$ exciting the j -th scatterer is known after defining an effective propagation constant K which is a complex ($K = K_1 + i K_2$). Following this definition, the average or effective exciting field $\langle \alpha_n^j \rangle_j$ can be written as

$$\langle \alpha_n^j \rangle_j = A_n e^{iK k_0 \cdot r_j} \quad (9)$$

where k_0 is the propagation direction of the incident wave. The effective propagation constant K is obtained by solving the dispersion equation which is explained in detail in our previous papers. The unknown effective exciting amplitude A_n , however, can be solved by invoking the extinction theorem and is generally in the following form for spherical scatterers, for which the T-matrix is diagonal

$$A_n = [1 - 3/2 c (-1)^n \sum_{n'} T_{n'n} A_{n'}] [(ka^3) (K/k + 1)] \quad (10)$$

provided a spherical scatterer in an effective medium is considered. In Eq. (8), c is the volume concentration, a is the radius of the scatterer and k is the wave number in the host medium.

If we substitute Eqs. (8) and (9) in (5), we obtain

$$\begin{aligned} \langle |u|^2 \rangle = & n_0^2 \iint [g(r_j - r_k) - 1] \sum_{n'} T_{nn'} \langle \alpha_n^j \rangle_j \sum_{n''} T_{nn''}^* \langle \alpha_{n''}^{k*} \rangle_k dr_j dr_k \\ & + n_0 \int \sum \sum T_{nn'} \langle \alpha_n^j \rangle_j^* dr_j \end{aligned} \quad (11)$$

We notice that in Eq. (11), the multiplication of the T-matrix and the effective exciting field is

independent of the integral and the pair correlation function. In fact, the integral of the pair correlation function turns out to be the Fourier transform of the radial distribution function $[g(\mathbf{x})-1]$. This fact further simplifies the numerical computation of the incoherent intensity. In order to investigate the contribution of the incoherent intensity, we calculate two major normalized quantities which are defined as follows:

(i) Normalized incoherent Intensity $\langle I' \rangle$ in the far field

$$\begin{aligned} \langle I' \rangle &= (I_s/I_0) (kr)^2 (v/V) \\ &= 2c(\sum T_n A_n Y_n)(\sum T_n'' A_n'' Y_n'')^* F(\mathbf{k}_0, \mathbf{K}, \mathbf{r}) / (K_2/k)(ka)^3 (Z/a) \end{aligned} \quad (12)$$

where Y_n are the normalized spherical harmonics, $(Y_{lm\sigma}(\theta, \phi))$, Z is the distance of penetration of the incident wave, n' is the index representing l and m ; r is the radial distance from the center of the scattering region to the observation point, v is the volume of a single scatterer and V is the whole scattering volume (region). The function F in Eq. (12) is given below

$$F = 1 + n_0 \int [r g(\mathbf{x})-1] \exp [i(\mathbf{K}\mathbf{k}_0 - \mathbf{k} \mathbf{r} / r) \cdot \mathbf{x}] dx \quad (13)$$

RESULTS AND DISCUSSION:

In order to study the characteristics of the incoherently scattered wave intensity, we choose electromagnetic waves as probing waves simply because there are a number of applications in remote sensing. Recently, there have been efforts to explain the so called backscattering enhancement both experimentally and analytically. Although several attempts have been tried to explain the phenomenon, we think the major contribution toward a locally high incoherent intensity in the backscattering direction may depend more on Mie scattering and less on the concentration of scatterers. Besides, the properties of different scatterers do affect the scattering characteristics and the backscattering enhancement relies heavily on the albedo of a single scatterer. We are going to explain this later by using several of our numerical results.

By sending plane electromagnetic waves through scatterers we intend to find, first, the

angular dependence of the incoherent intensity and the influence from different polarizations, e.g., vertical and horizontal polarizations. If it is not specifically mentioned, scatterers are assumed to be spherical ice particles with a relative dielectric constant $\epsilon = 3.168$ embedded in air. Figure 1 presents the normalized incoherent intensity versus observation (scattering) angles. The forward scattering angle is, in our case 0° and therefore the backscattering direction is at 180° . The nondimensional frequency considered is 0.6 which is equivalent to a physical frequency of about 14 GHz if a 2 mm particle is considered.

After the electromagnetic waves travel about 1 km, we can see that the scattered incoherent intensities in all directions are very small compared to that of the coherent wave (or the coherently transmitted wave). As a matter of fact, this is true for all incoherently scattered intensities. From the field investigation as well as from the controlled experiments, incoherent signals are usually 25-50 dB or even more down from the coherent signal. But as we discussed in the previous section, this does not imply that the incoherent signals are unmeasurable.

Taking a further look at Fig. 2, we can conclude that the vertical polarization gives more angular dependence of the incoherent intensity than the horizontal one. There is an extremely low intensity (i.e., a deep minimum in the curve) that occurs at 90° at a $ka=0.6$. This phenomenon happens again, however, at a higher observation angle of 125° when the frequency ka is raised to 2. There is no polarization difference at the forward and backscattering directions for the incoherent intensities.

Numerical results for the normalized incoherent intensity versus frequency for different concentrations at the backscattering direction are presented in Fig. 3. The scattered intensities are vertically polarized. As can be seen from the figure, locally low intensities happen, for all concentrations, at $ka=1.5$ which is a resonant frequency for ice particles. Besides the magnitudes of the intensities, one is able to find that the minimum is wider when the concentration is smaller. The difference in the magnitudes of the intensities is quite noticeable in the frequency range from $ka=0.7$ to 1.5.

In Figs. 4 and 5, we compare the backscattered intensity calculations with and without the effect of pair correlations. These results tell us that if the intensity is calculated without considering the pair correlation function when the concentration becomes even moderately high, i.e., 5%, one is able to see the difference in the magnitude particularly in the low frequency range. This is valid for both vertical and horizontal polarizations.

The scatterers in the host medium are actually excited by waves with the effective exciting amplitudes which result from different orders of scattering. One way to consider the order of scattering is by perturbing the incident wave amplitude which, in our case, is unity. Therefore, in Fig. 6, we present results from calculating incoherent intensities using different exciting amplitudes and the difference is quite noticeable when the frequency is high, especially at the resonant scattering frequency.

Figure 7 is another representation of the backscattered intensity versus frequency. However, the dependence of the intensities on concentrations is clearer using the backscattering coefficient computation. The bistatic scattering coefficient has a strong angular dependence under different frequencies and is shown in Fig. 8.

In order to understand the effects of multiple scattering on the incoherent intensity and its final characteristics, the study of the scattering response from a single scatterer proves to be very informative. First, we examine the differential scattering cross section for an ice sphere at low and high frequencies. The extremely low intensity occurring at 90° in Fig. 1 and can be explained by the polar plot of bistatic scattering cross sections in Fig. 9. At high frequencies, the intensity has a strong lobe in the forward direction and is highly directional in the range of about $\pm 10^\circ$. However, if a perfect conducting sphere is considered as a scatterer, at low frequencies, we can see from Fig. 11 that the forward scattering is about four times smaller than the backscattering. Furthermore, the scattering cross section is not zero at 90° . This means that the material properties of different scatterers dominate the final scattering characteristics. Therefore, even at the same observation angle, a particular phenomenon that occurs for one group of

scatterers may not occur for another group of scatterers with different properties.

The characteristics of the multiply scattered incoherent intensity has its similarity with that of the differential cross section of a single scatterer and can be again found in Figs. 12 and 13 when compared with Figs. 1 and 2. Figure 14 is a different representation of the polar plot in Fig. 10 but detailed magnitudes with respect to the observation angles are given. In addition, the difference between the vertical and horizontal polarizations is shown in the figures.

Different scatterers have a different albedo when illuminated by waves with different frequencies. Since the incoherent scattering characteristics depends heavily on the albedo of a single scatterer, Figs. 15 and 16 present the differential scattering cross sections versus scattering angles for an ice particle in air, a perfect conducting sphere in free space and a glass sphere in distilled water all excited by plane waves of two different frequencies, i.e., $ka=0.6$ and 7.28 . Indeed, we can see the property dependence and some behavior related to the incoherent scattering may be explained from these figures.

The differential cross section of a single scatterer also has a noticeable frequency dependence. In Fig. 17, we observe that the resonant scattering is different for different scatterers. For an ice sphere in air it happens at $ka=1.5$ while it shifts to a higher ka ($=1.6$) for a glass sphere in water. This implies that extra information is always available if we pay attention to the details of the frequency spectrum of the incoherent intensity.

Finally, we want to say something about the effect of the pair correlation function. In order to tell the importance of its effect on the final scattered intensity, we simply calculate the function F which appears in Eq. (12) and has been defined in Eq.(13). As can be seen from Eq. (12), it involves a Fourier transform of the pair correlation function and it contains an effective propagation constant K and hence depends on the properties of the scatterers, the concentration, frequency and angle of observation. However, in Figs. 18, 19 and 20, we can see that the Fourier transform of the pair correlation function dominates the scattering response particularly in the low frequency range and in the forward direction. In the high frequency range, it does not

affect the scattered intensity much. Also, we observed that the intensity decreases after a volume fraction $c = 15\%$, which is also a fact pointed out in Kuga's experiments. One is therefore able to conclude that when the frequency is high the magnitude of the scattered intensity is more dominated by Mie scattering as shown in Fig. 16. At low frequency, the backscattering enhancement cannot be observed especially for low concentrations of scatterers. Even if the concentration of scatterers is increased, no backscattering enhancement at the low frequency range can be observed.

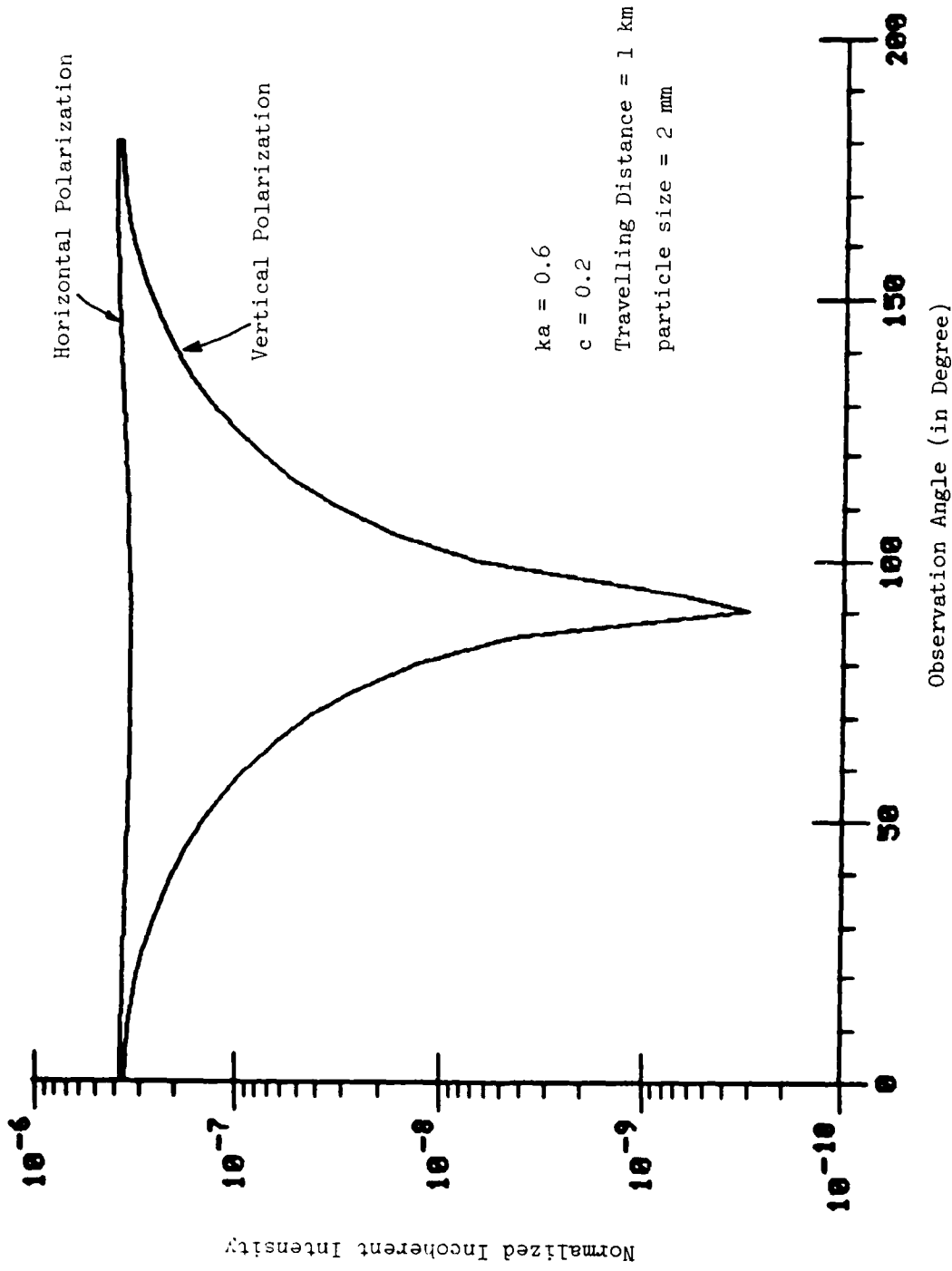


Figure 1. Normalized incoherent intensity vs. observation angle.

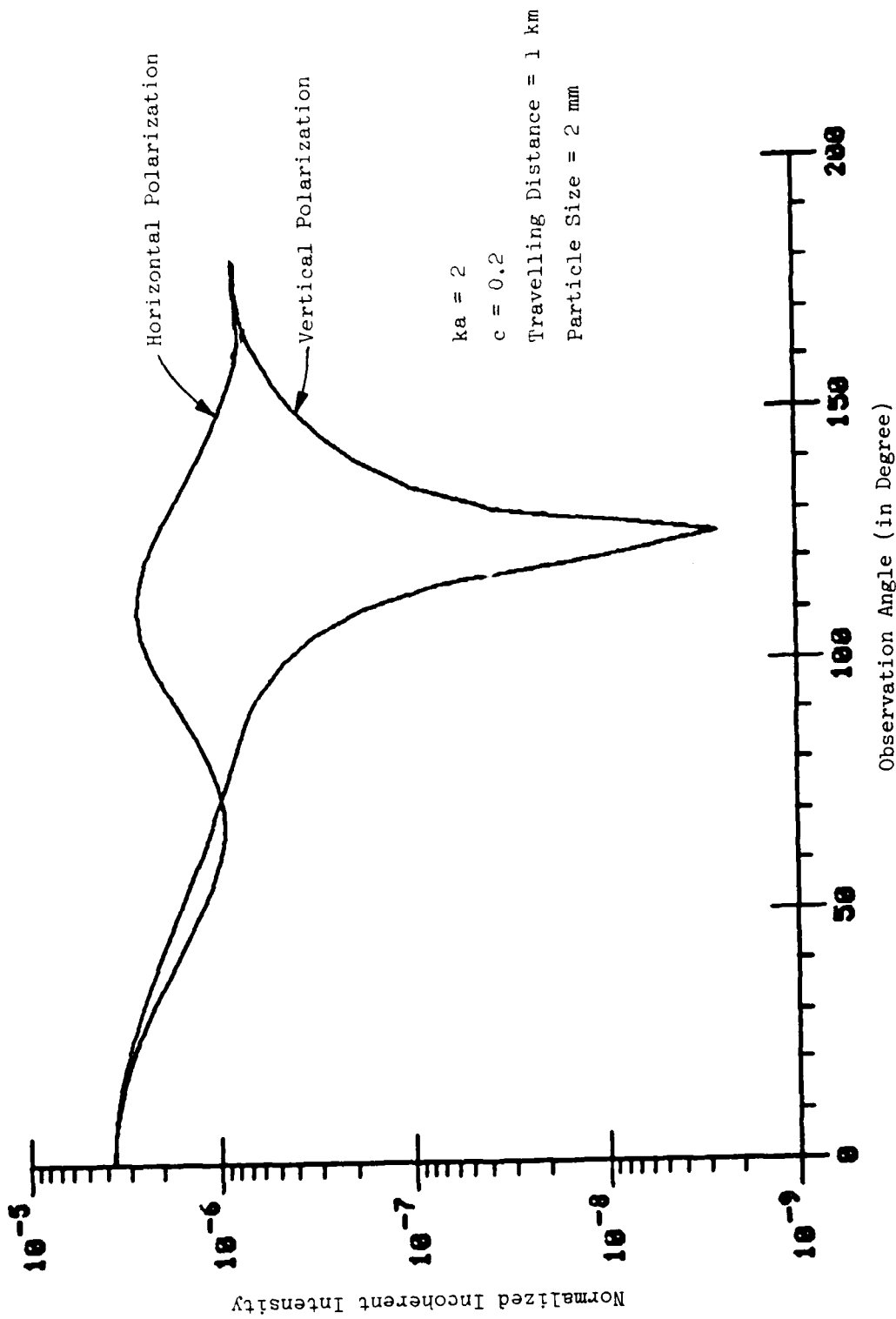


Figure 2. Normalized incoherent intensity vs. observation angle.

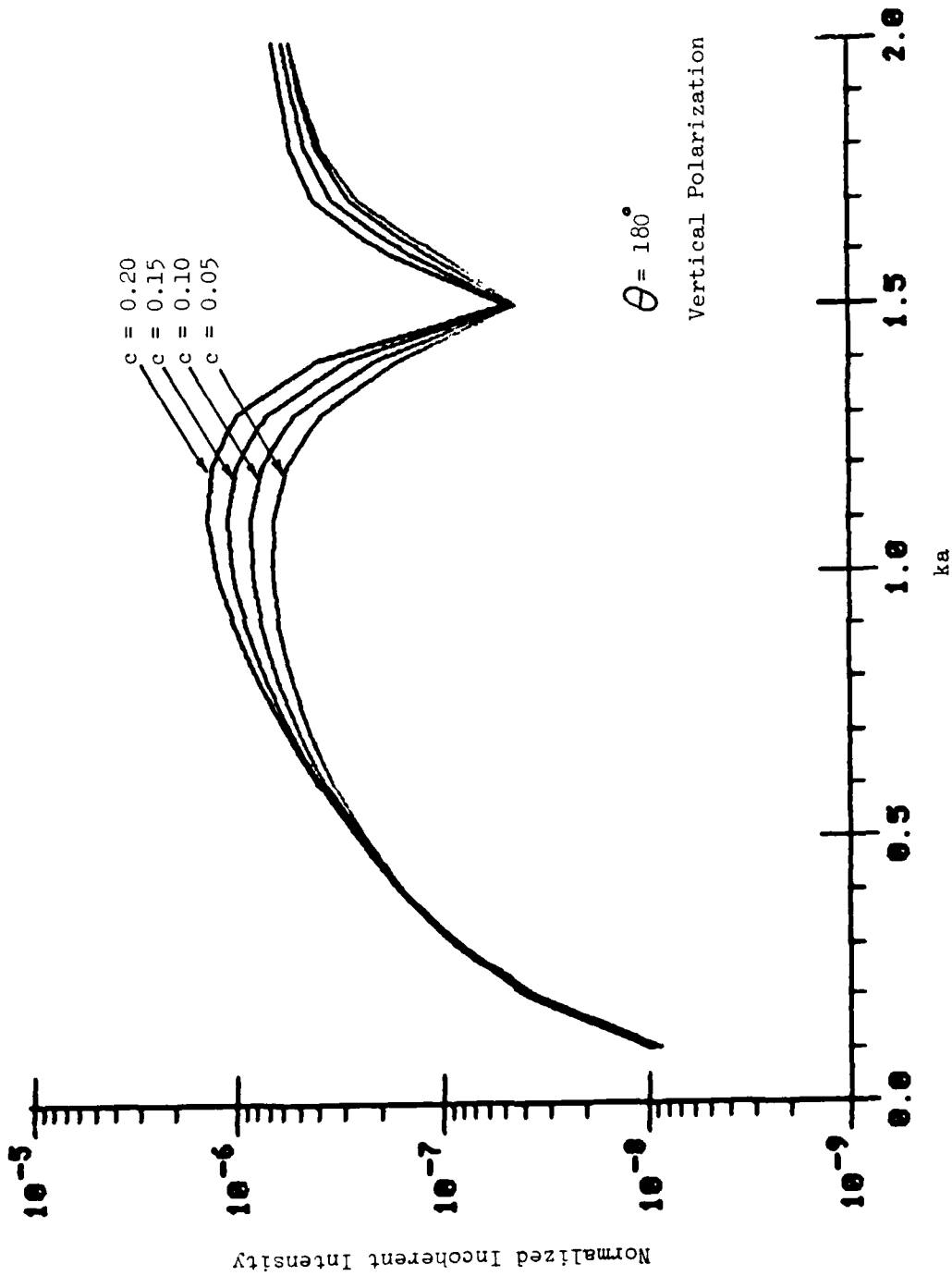


Figure 3. Normalized incoherent intensity vs. nondimensional frequency.

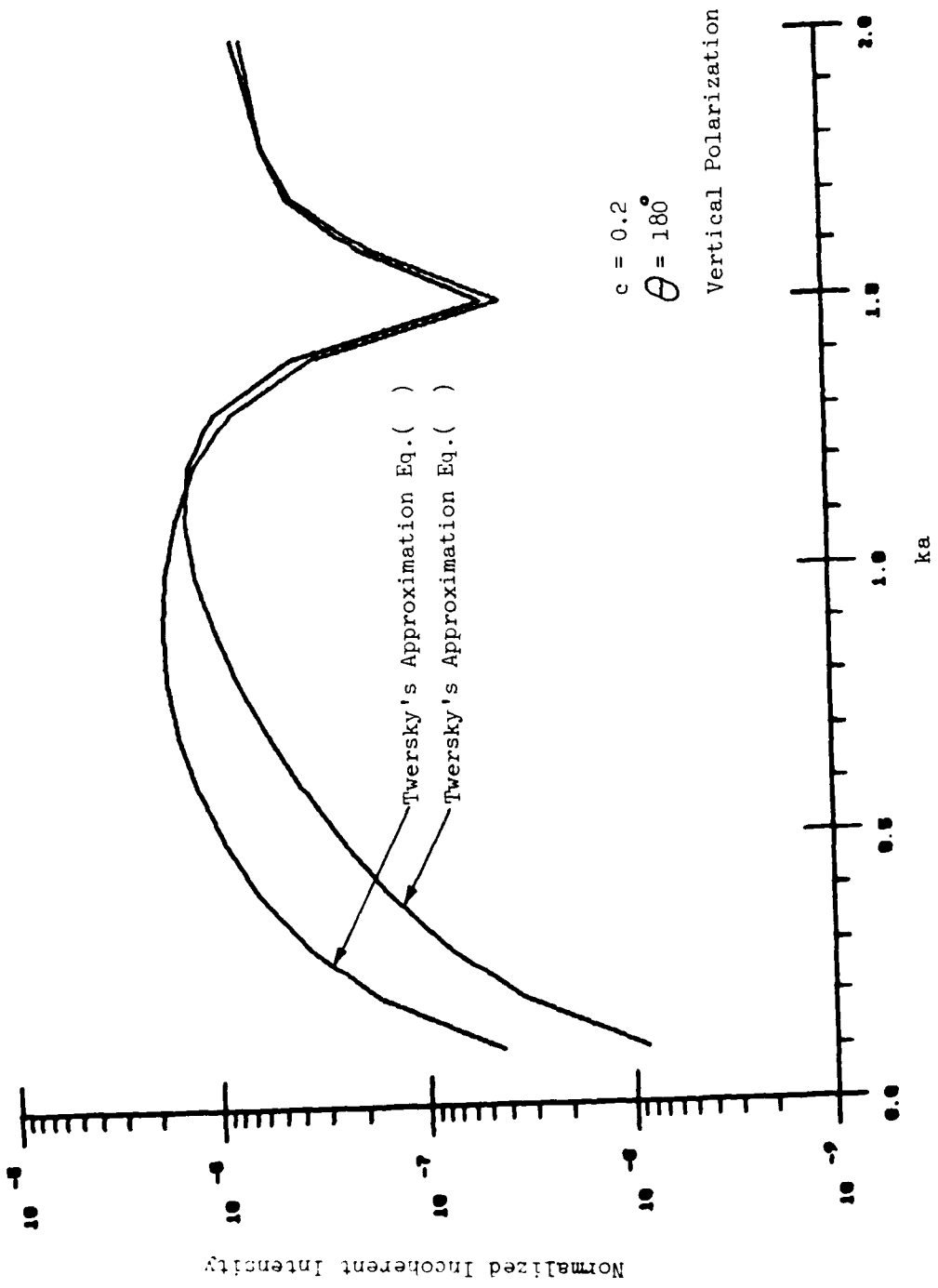


Figure 4. Normalized incoherent intensity vs. nondimensional frequency.

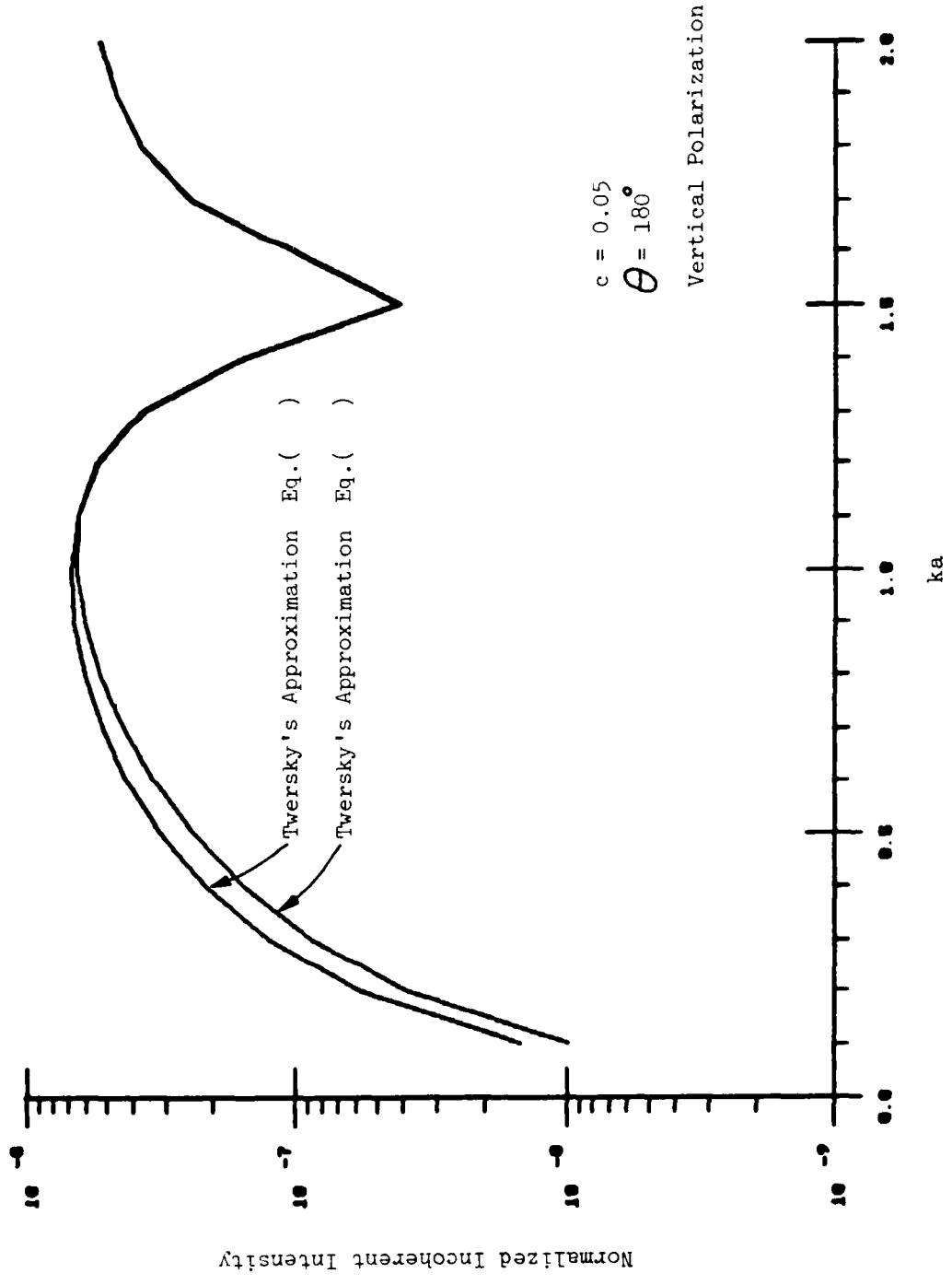


Figure 5. Normalized incoherent intensity vs. nondimensional frequency.

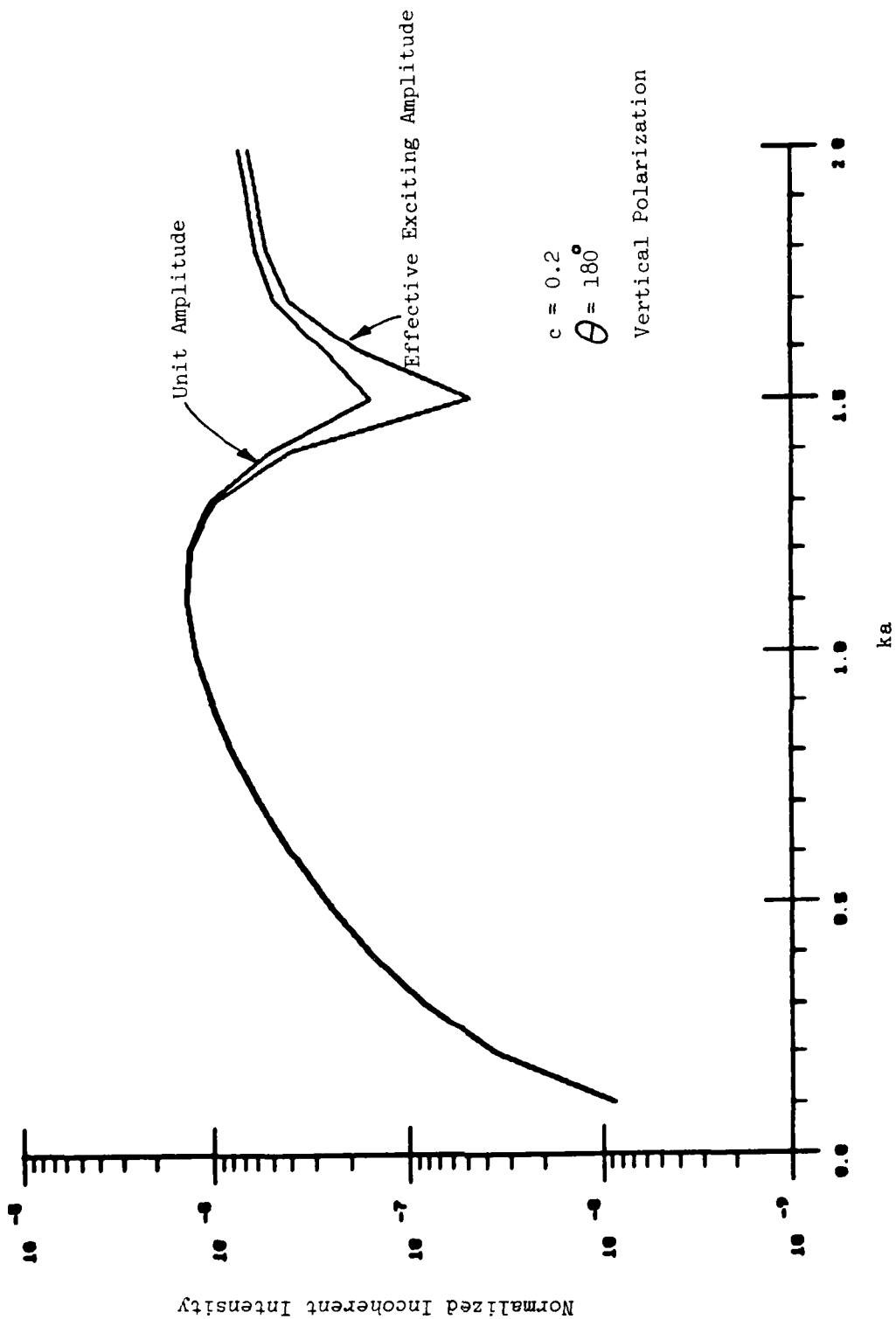


Figure 6. Normalized incoherent intensity vs. nondimensional frequency.

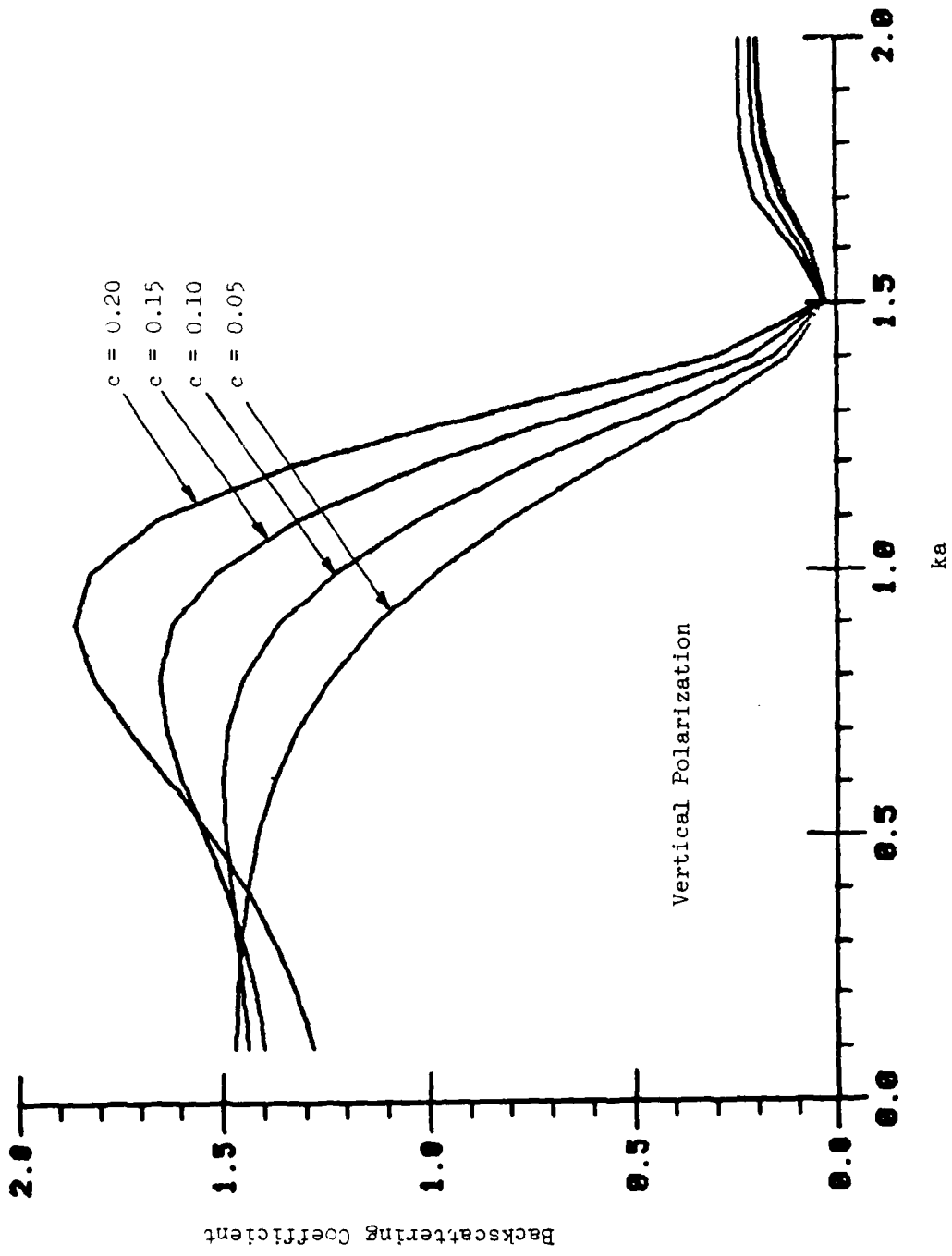


Figure 7. Backscattering coefficient vs. nondimensional frequency.

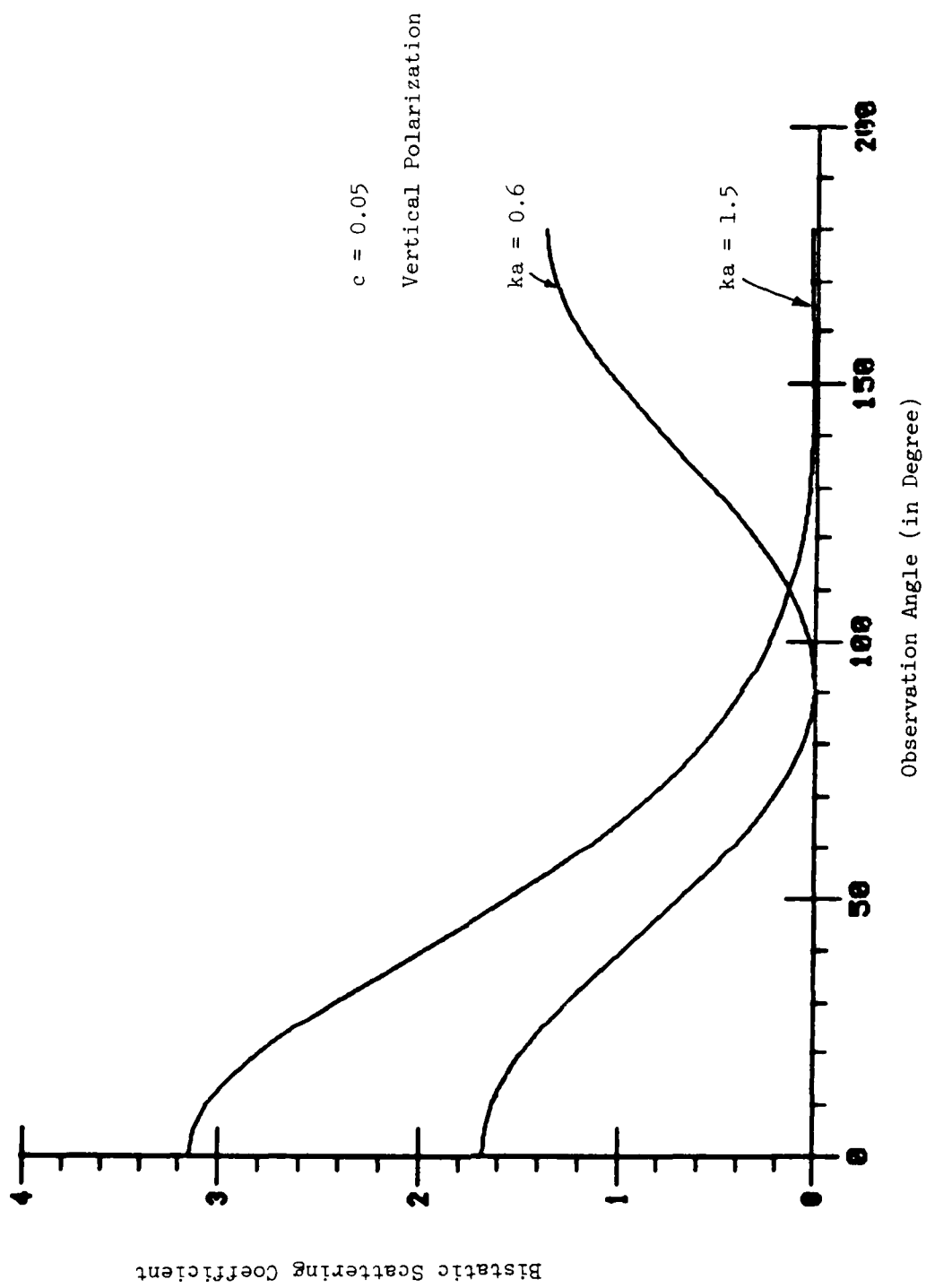


Figure 8. Bistatic scattering coefficient vs. observation angle.

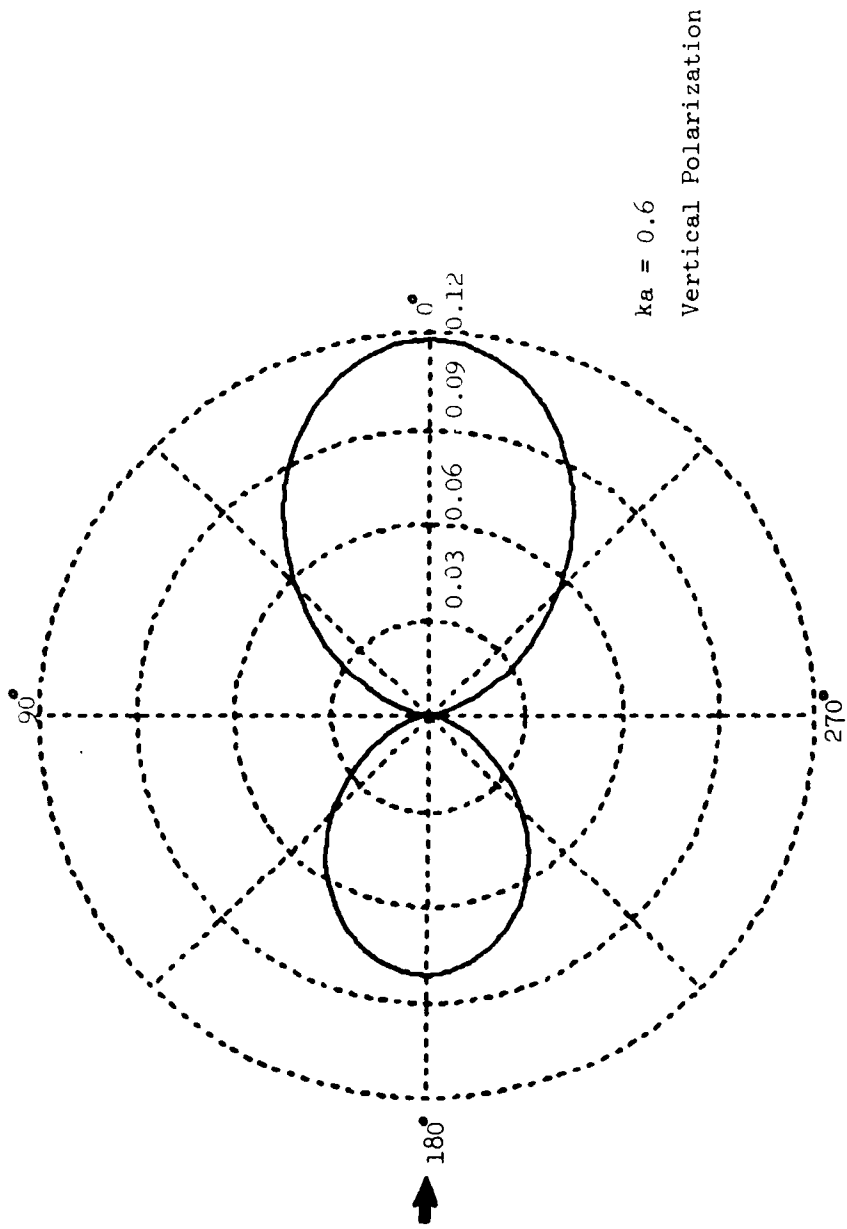


Figure 9. Polar plot of bistatic scattering cross section.

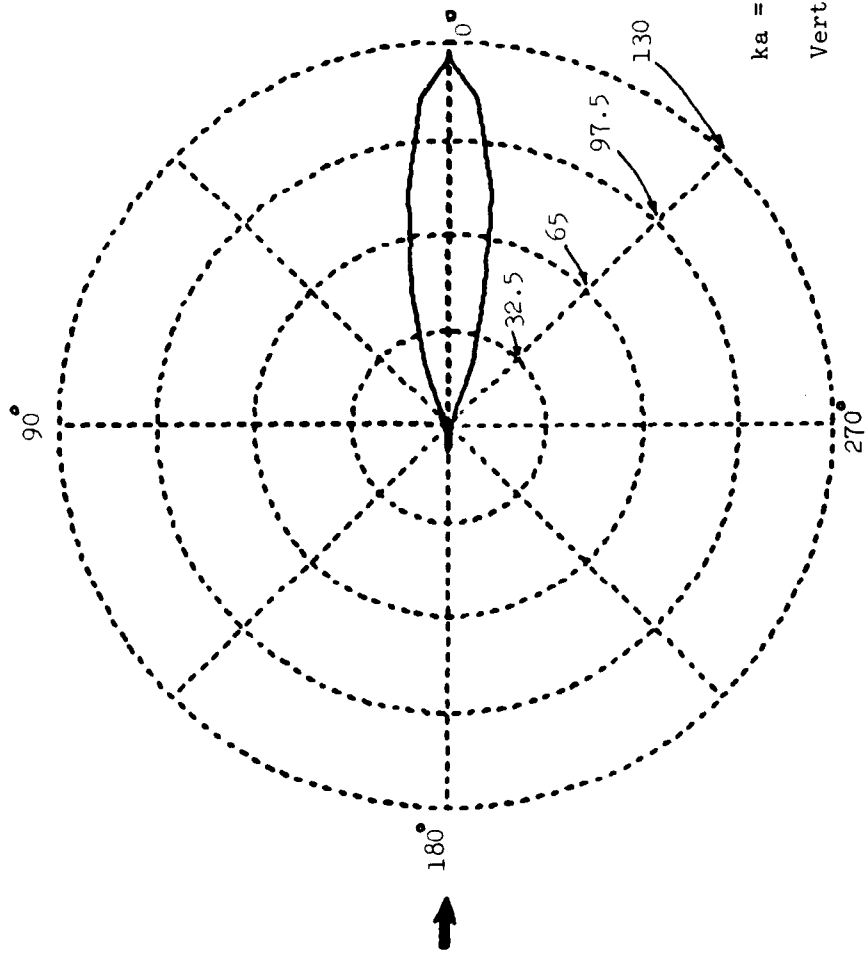
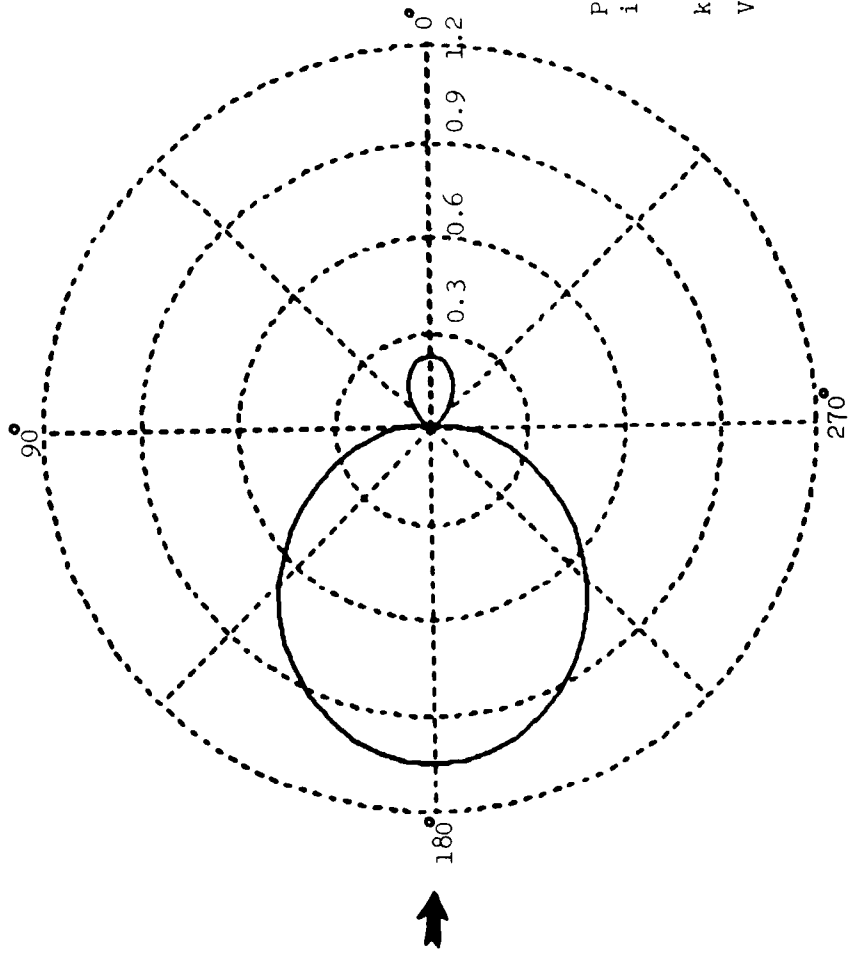


Figure 10. Polar plot of bistatic scattering cross section.



Perfect Conducting Sphere
in Free Space

$ka = 0.6$

Vertical Polarization

Figure 11. Polar plot of bistatic scattering cross section.

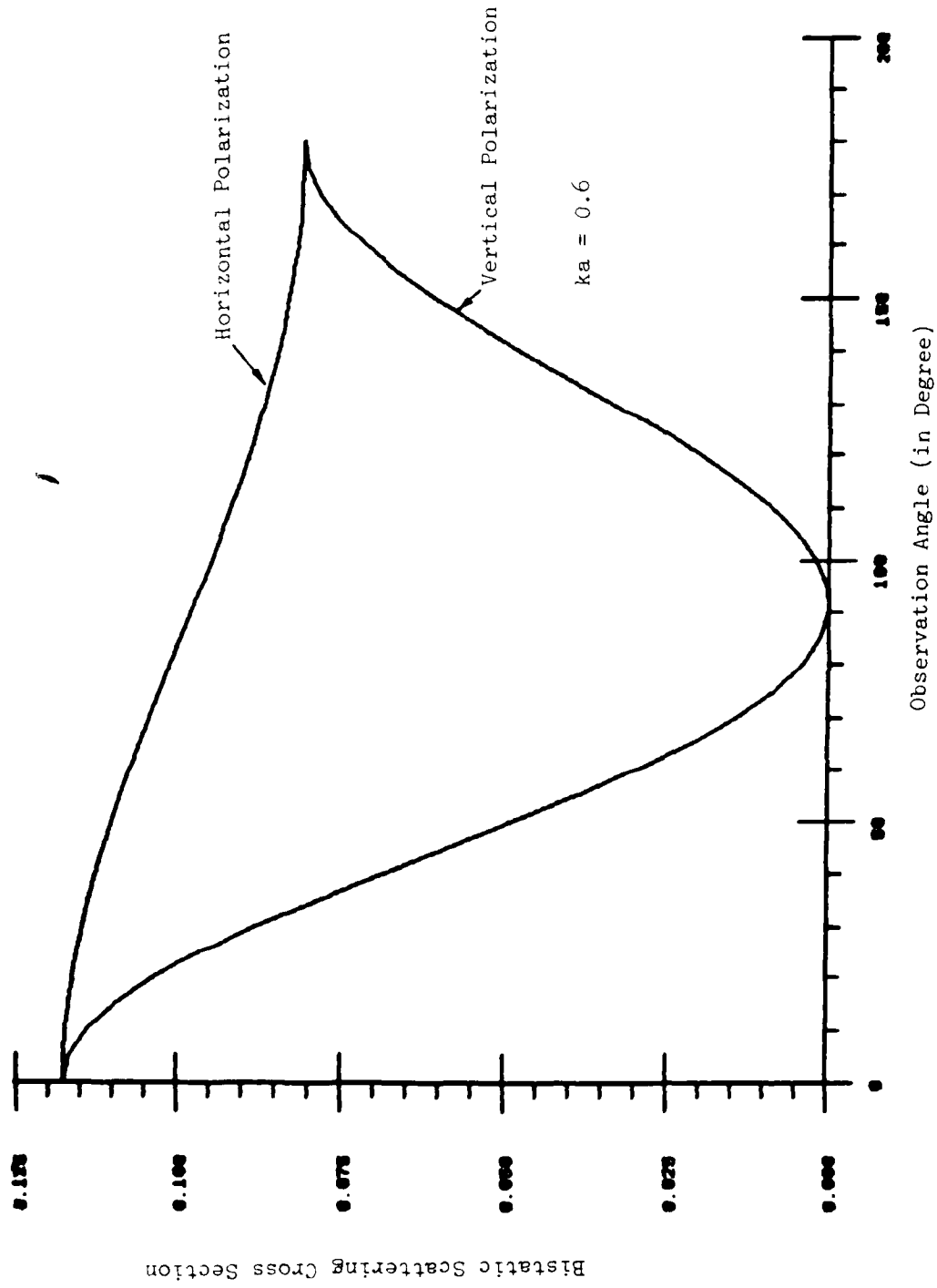


Figure 12. Bistatic scattering cross section vs. observation angle.

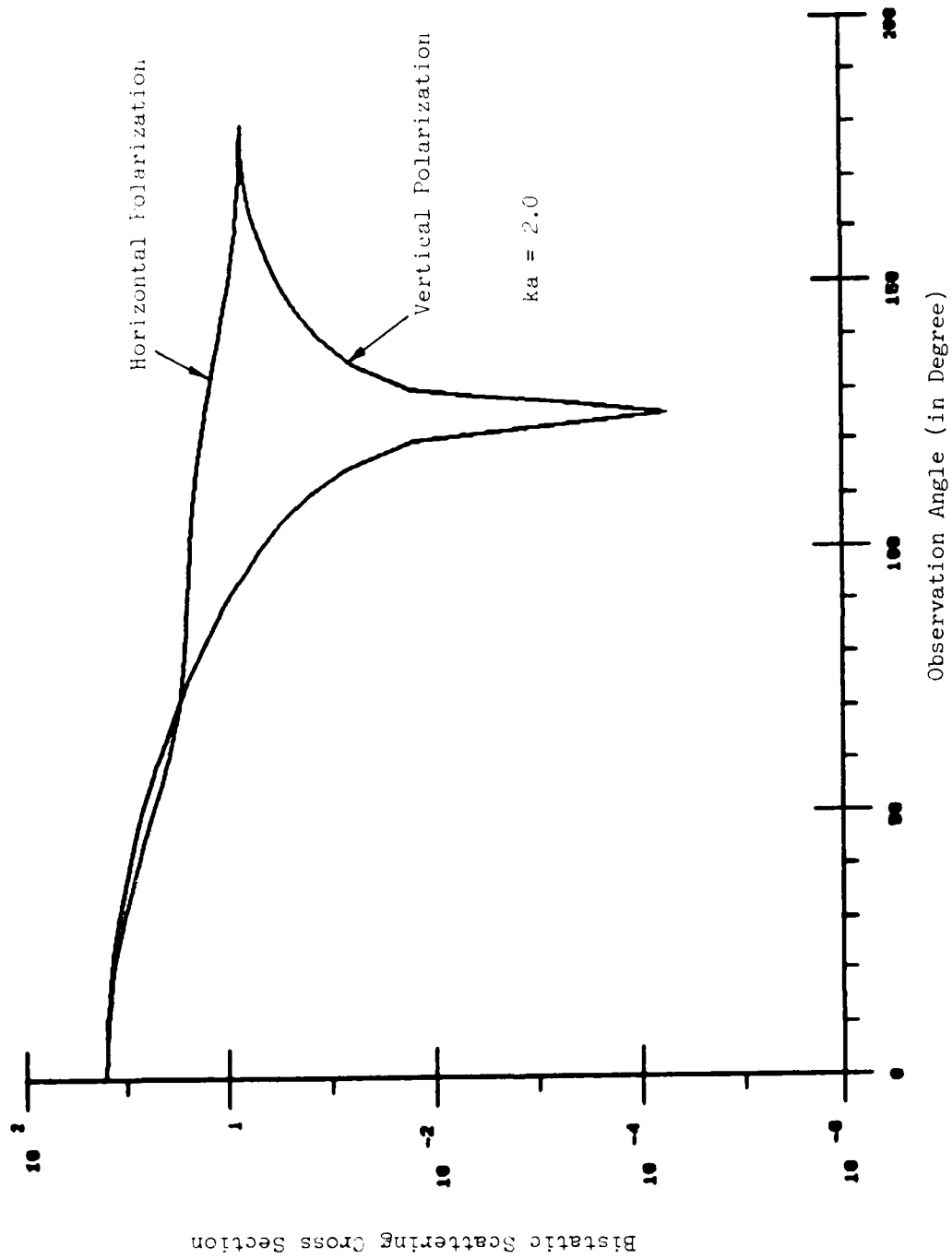


Figure 13. Bistatic scattering cross section vs. observation angle.

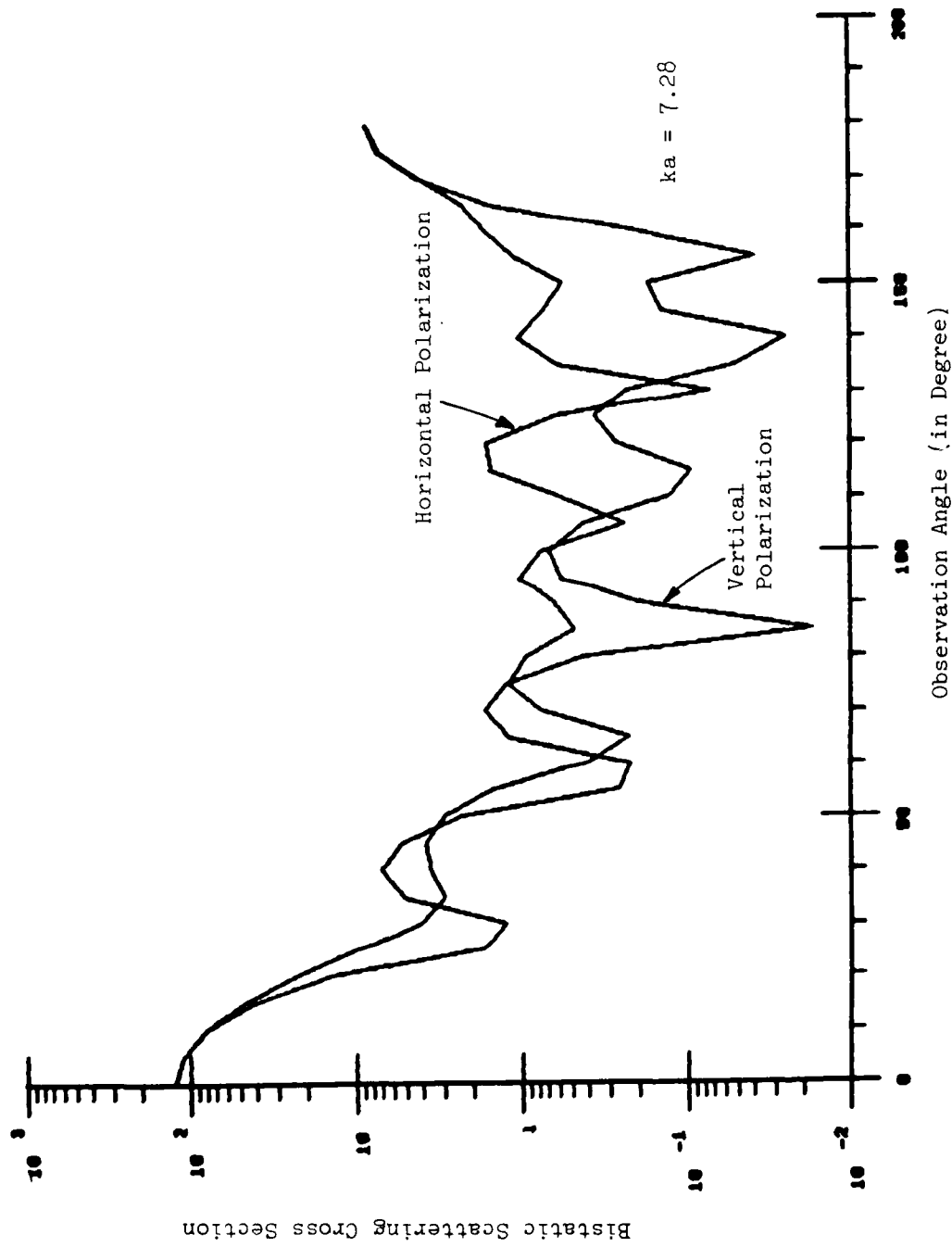


Figure 14. Bistatic scattering cross section vs. observation angle.

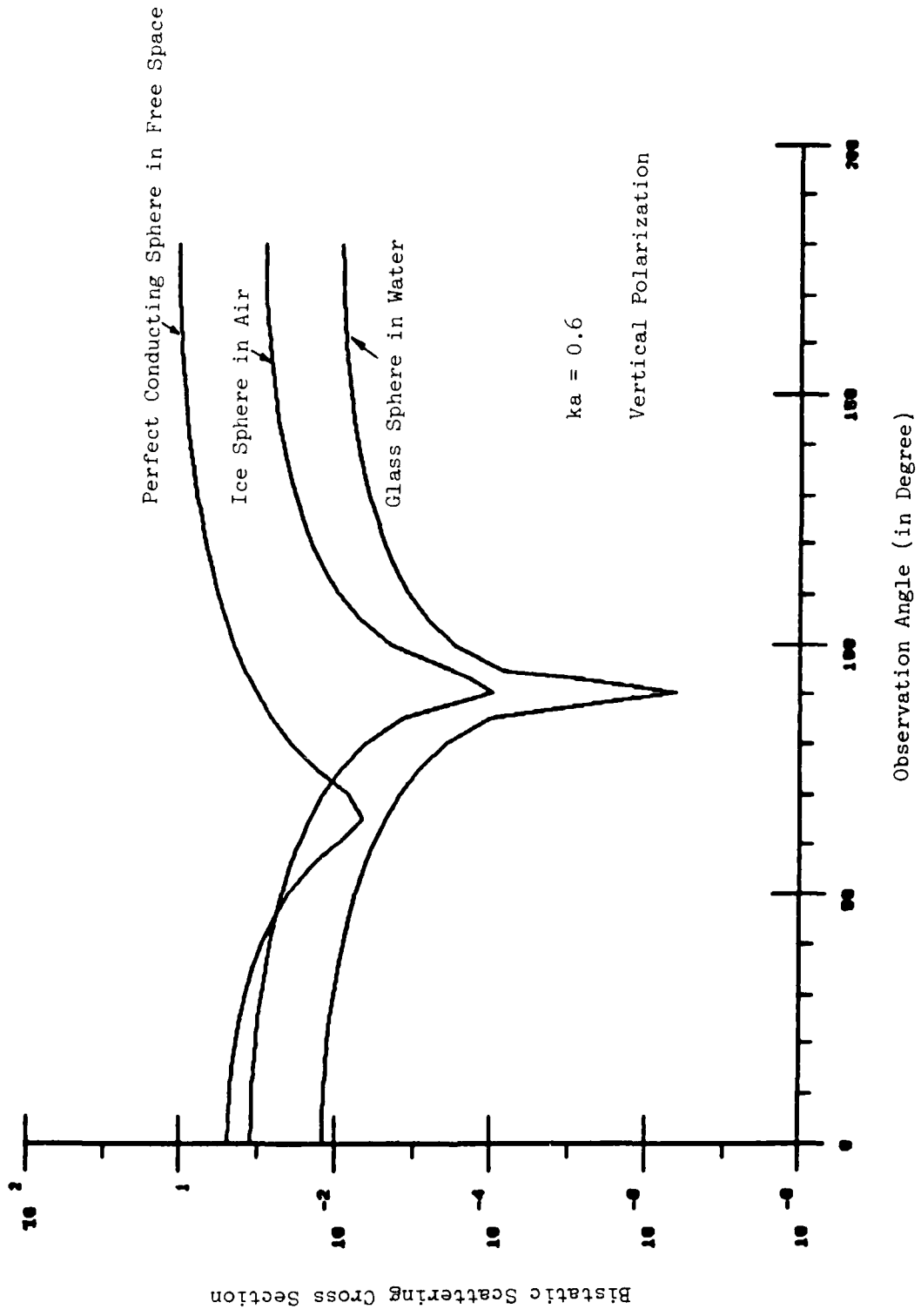


Figure 15. Bistatic scattering cross section vs. observation angle.

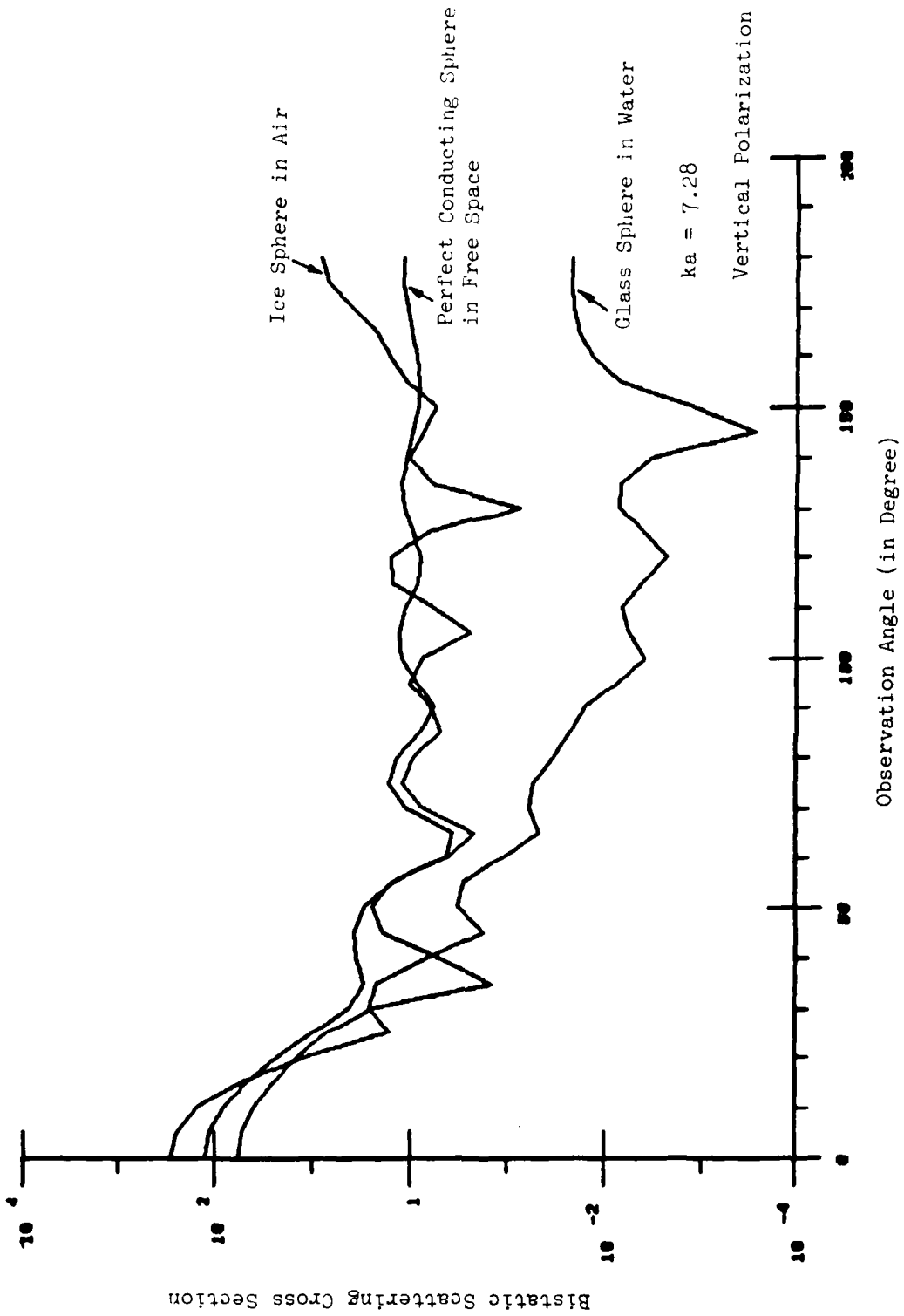


Figure 16. Bistatic scattering cross section vs. observation angle.

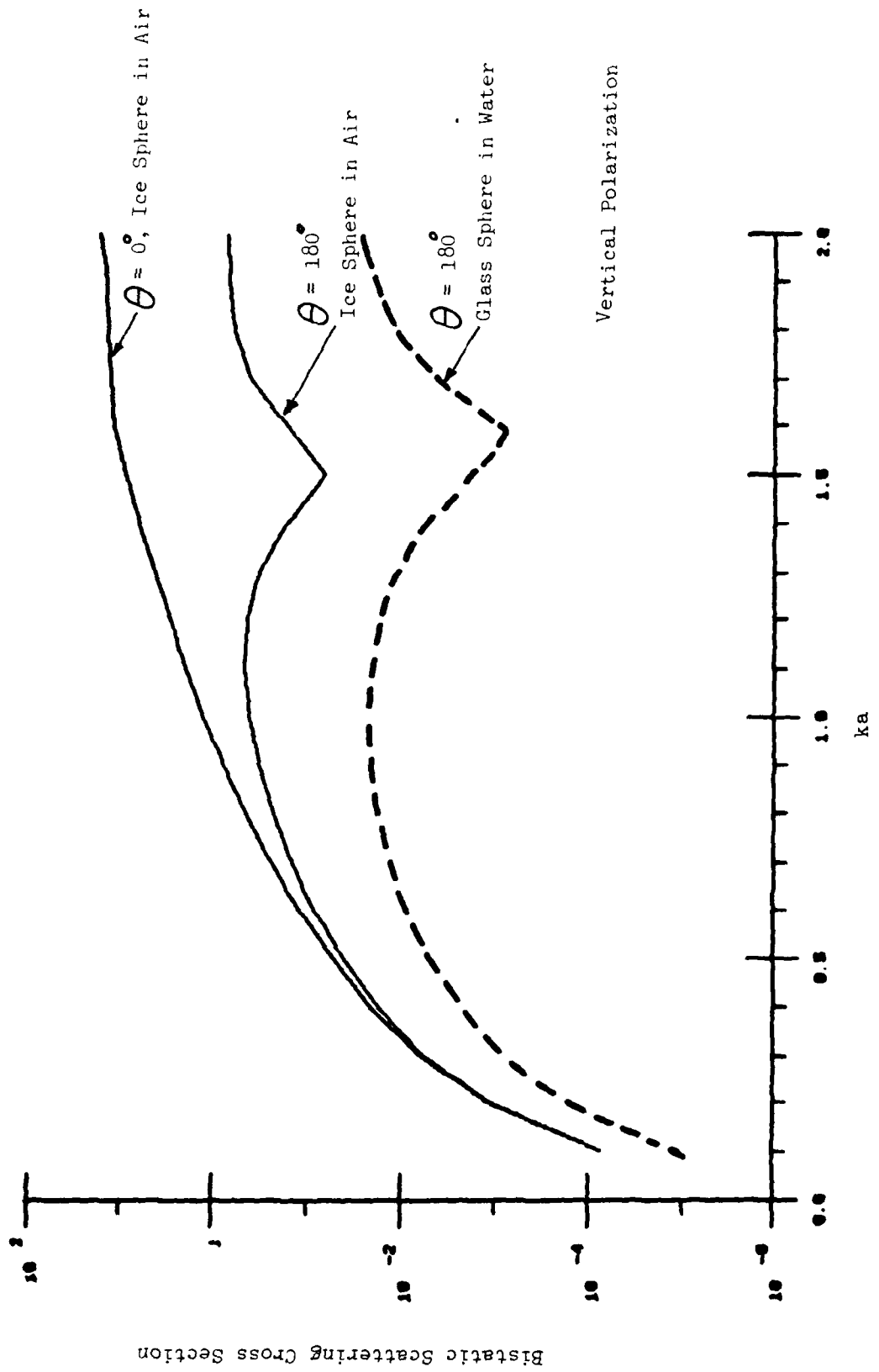


Figure 17. Bistatic scattering cross section vs. nondimensional frequency.

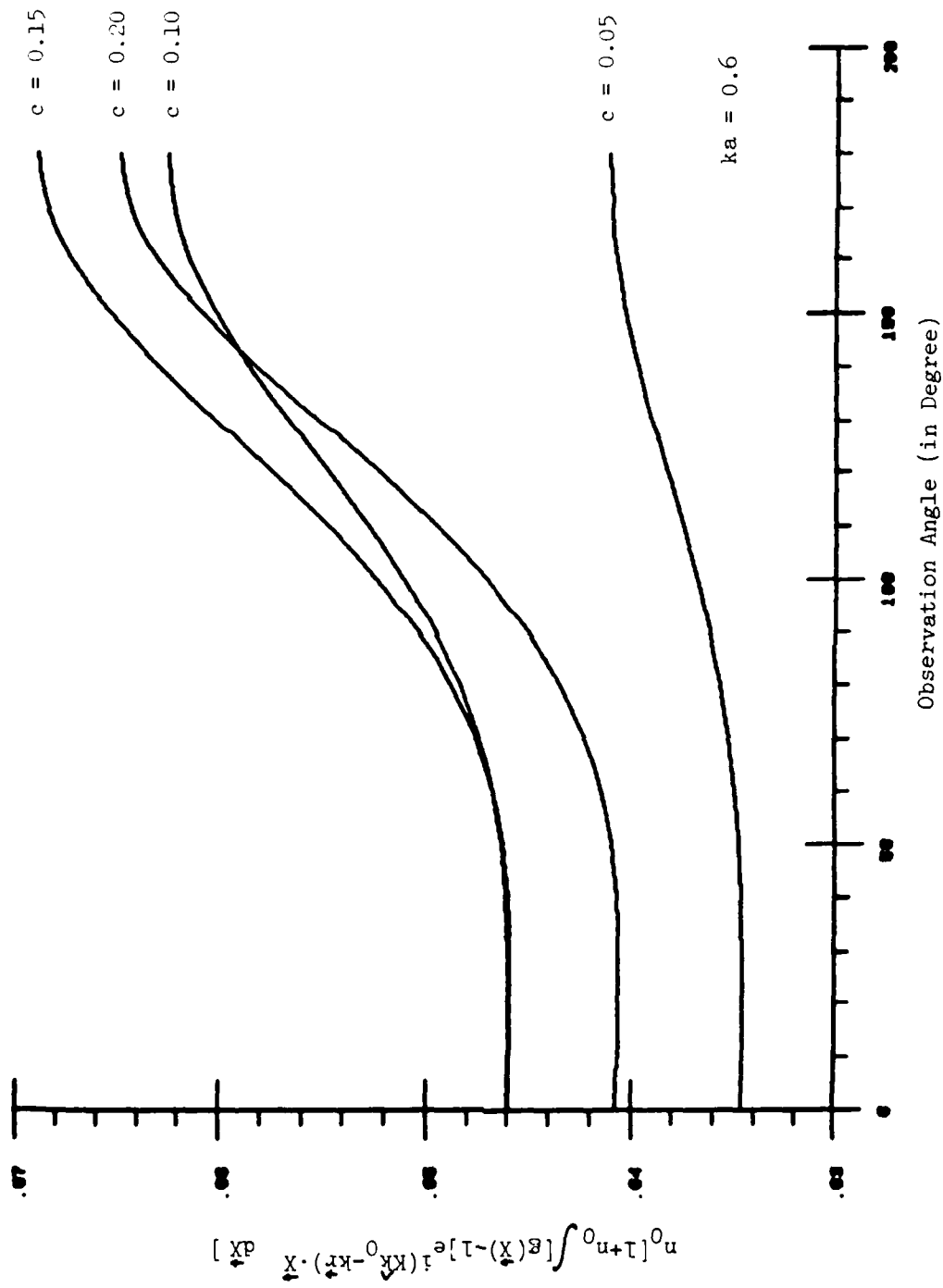


Figure 18. Effect of pair correlation function vs. observation angle.

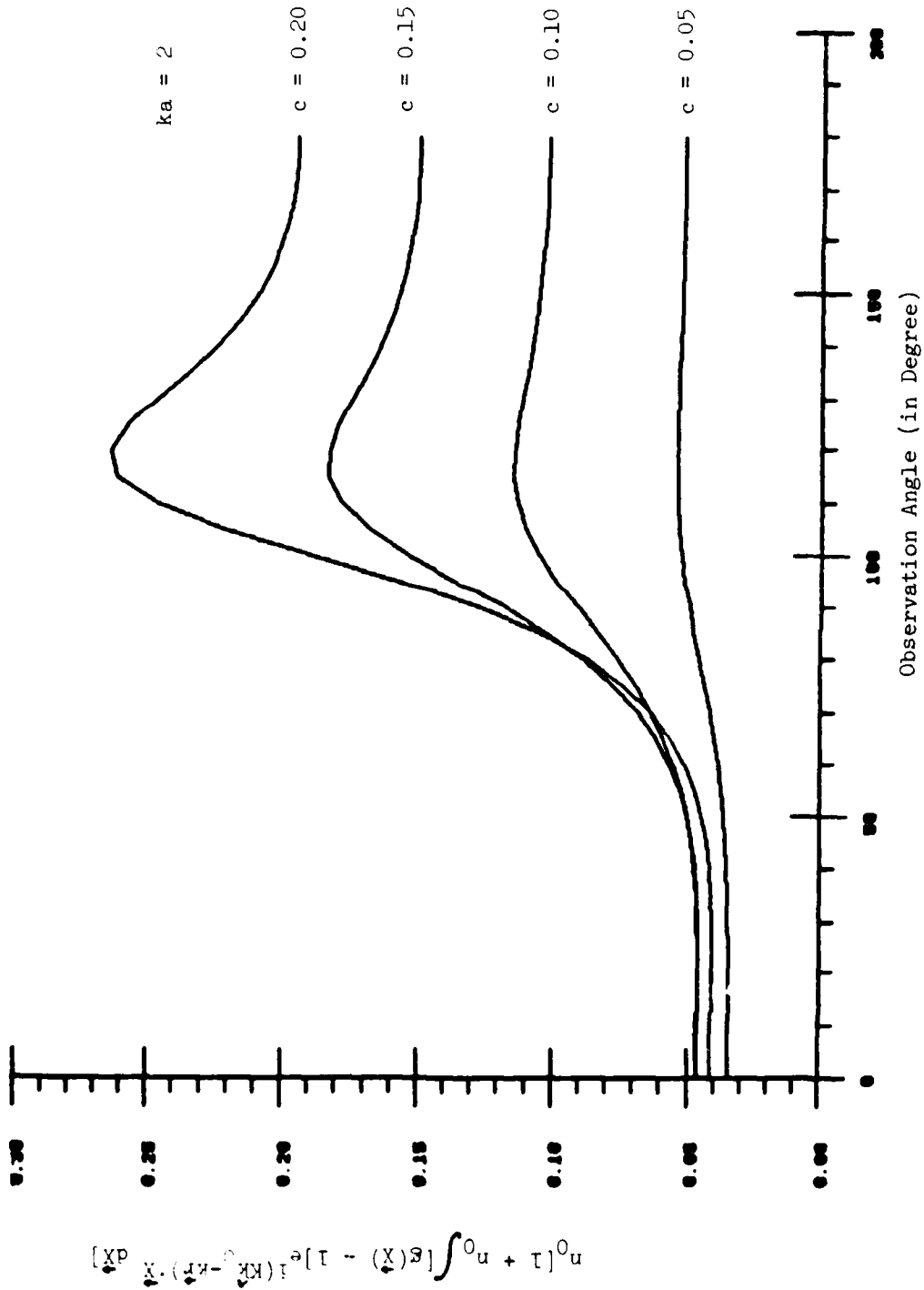


Figure 19. Effect of pair correlation function vs. observation angle.

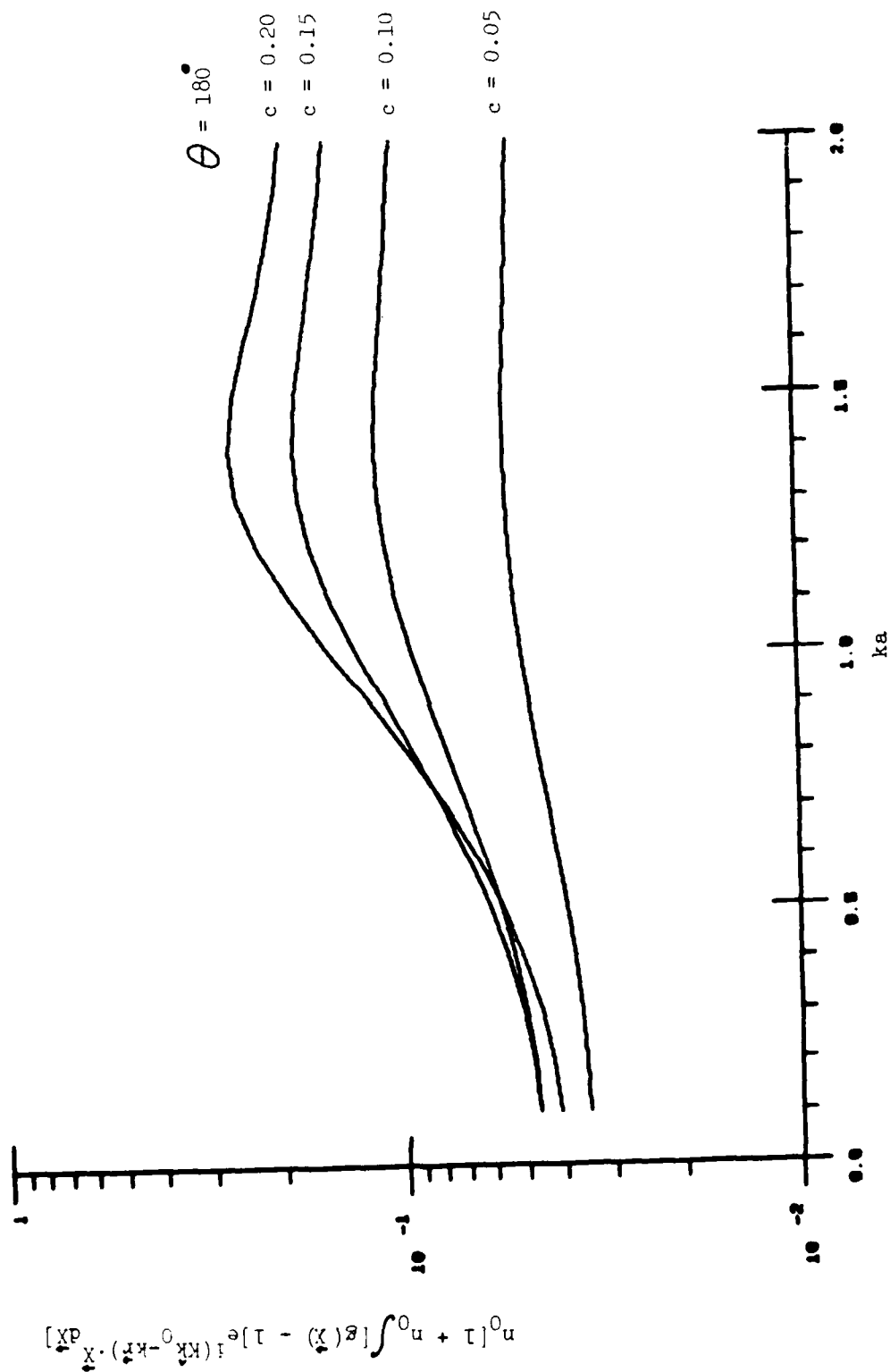


Figure 20. Effect of pair correlation function vs. nondimensional frequency.

END

FILMED

4-86

DTIC